Chapter 4

New Insights into Amorphous Macromolecules and Their Mixtures from Advanced Magnetic Resonance Experiments

Jeffery L. White,*[,1] Marcin Wachowicz,[1] Lance Gill,[1] Joshua Damron,[1] and Justyna Wolak-Dinsmore[2]

[1]Department of Chemistry, Oklahoma State University, Stillwater, OK 74078
[2]Department of Chemistry, North Carolina State University, Raleigh, NC 27695-8204
(Current address: Liposciences, Inc., Raleigh, NC)
***E-mail: jeff.white@okstate.edu**

Amorphous blends of high molecular weight macromolecules present some uniquely challenging problems in structure-function investigations, and pose some interesting fundamental questions regarding dynamics and thermodynamics. In the absence of ordered morphologies or extensive isotopic labeling, traditional diffraction and spectroscopic techniques may not provide component-specific information. In this contribution, we review experimental methods which have been developed to specifically probe the dynamics and thermodynamics of mixing in amorphous blends. Our approach is based on advanced NMR techniques that provide chain-specific data over a wide temperature range without introduction of any isotopic labeling or probe molecules.

Introduction

The science related to polymer blends has historically enjoyed a productive marriage between intellectual pursuit and economic utility, as recently discussed in a national workshop hosted by the National Science Foundation (*1*). The notion that the polymer blend area is a mature science can be challenged by simply assessing the lack of understanding surrounding mixtures of amorphous

In NMR Spectroscopy of Polymers: Innovative Strategies for Complex Macromolecules; Cheng, H. N., et al.; ACS Symposium Series; American Chemical Society: Washington, DC, 2011.

macromolecules of even the most simple chemical structure. As the polymer science community, both from an intellectual and engineering motivation, pursues increasingly complex systems, tailored composites, hybrid and hierarchical structures, self-assembly, and biologically inspired materials as outlined in a recent *Macromolecules* "Perspectives" article (*2*), we find that the same key questions that characterize problems in mixtures of amorphous polymers continue to arise in these emerging interdisciplinary areas. For example, simply measuring with confidence the length scales within which two polymers are mixed in a binary mixture of two non-crystalline macromolecules can be very challenging, even for very simple polymer chain architectures. Also, what causes amorphous mixtures to have a homogeneous, intimately mixed arrangement of its constituent chains versus a heterogeneous, phase separated morphology? If intimate mixing of the two polymer species occurs, does this mean that the chains assume new "identities" relative to their pure component characteristics, and if so, in what ways? Can we synthetically manipulate the macroscopic properties of the end-result blend by systematic variation of chemical structure? Amorphous polymer blends, which for the purposes of this contribution mean mixtures of high polymers with no crystalline regions in the final blend, represent the first step in generating complex polymer systems. As such, fundamental understanding of how they behave, and connections between microscopic structure versus end-use properties is paramount to continued progress in key areas of macromolecular science, ranging from synthetic to engineered to biological materials. In addition, the science of "soft matter" is growing as an interdisciplinary focal point for researchers from physical, biological, and materials science areas (*3*), revealing an increasingly apparent need for rigorous experimental techniques capable of providing component-specific information in heterogeneous amorphous systems. We note in passing that much of the same language that has pervaded the polymer science community is now beginning to emerge in protein and enzyme science (*4*).

In this review, we will discuss experimental strategies developed to address key questions originally motivated by our interest in understanding miscibility in technologically important polyolefin blends, which are composed of completely saturated (i.e., only sp^3 carbons and hydrogens) high-molecular weight macromolecules. Since polyolefin blends have no chemical heterogeneity, they are very difficult to study with chain-level specificity in the absence of extensive isotopic labeling. In addition, they often are composed of chains with similar dipole moments, or no permanent dipole at all, and as amorphous mixtures, exhibit broad and diffuse glass transitions. Therefore, traditional methods like dielectric spectroscopy and differential scanning calorimetry are not generally applicable to amorphous polyolefin mixtures. As various polymer combinations were examined, we found that the selectivity inherent to our experimental approach based on variable-temperature CODEX[5] solid-state NMR experiments addressed many general questions in the current polymer blend literature related to thermodynamics of mixing, differential chain dynamics, time-temperature superposition, dynamic heterogeneity, and glass transition time-scales. Guiding principles for the strategies discussed here include: [1] Non-invasive access to quantitative chain-specific information before and after formation of mixtures;

In NMR Spectroscopy of Polymers: Innovative Strategies for Complex Macromolecules; Cheng, H. N., et al.;
ACS Symposium Series; American Chemical Society: Washington, DC, 2011.

[2] Data outputs in a format accessible to the general polymer science (i.e., non-NMR) community; [3] Experimental measures of average/mean chain behavior as well as heterogeneity/distributions in chain behavior; [4] Quantitative conclusions related to the thermodynamics of macromolecular mixing; [5] General applicability to amorphous materials. These will be discussed in the ensuing sections.

Experimental Section

Complete details for the synthesis, acquisition, and characterization of the polymers have been described (*6–9*). In general, all polymers used in our studies have molecular weights in the range 30,000 – 1,000,000, i.e., synthetic high polymers well above the entanglement molecular weight. The individual systems will be described in the text when appropriate, but include polymers and various binary blends composed of atactic polypropylene (aPP), head-to-head polypropylene (hhPP: made via anionic polymerization of dienes and hydrogenation), polyethylene-co-butene (PEB: monodisperse copolymer made via anionic polymerization and hydrogenation), polyisobutylene (PIB-a commercial material), polyvinylethylene (PVE: 88% 1,2-polybutadiene enchainment), and polyisoprene (PI: 97% cis-1,4 enchainment). Representative structures for the repeat units are shown in Scheme 1.

All systems were studied in bulk, i.e., without any solvents. Miscible blends (either equimolar or 50/50 wt%) were made by casting from solutions in a good solvent, and were exposed to vacuum pumping for several days prior to use. Characterization by TGA and ^{1}H NMR revealed that no residual solvent existed in any blend.

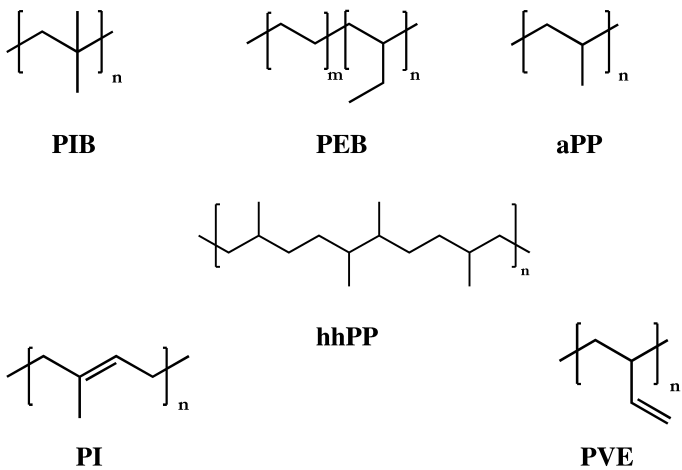

Scheme 1

In this review, we will primarily focus on an experimental strategy based on variable-temperature CODEX (Centerband-Only Detection of EXchange)

In NMR Spectroscopy of Polymers: Innovative Strategies for Complex Macromolecules; Cheng, H. N., et al.; ACS Symposium Series; American Chemical Society: Washington, DC, 2011.

experiments. However, several other experiments (including spin-diffusion measurements to verify miscibility, GPC, and DSC) were completed prior to CODEX analysis, as previously described (*7–9*). The CODEX experiment, first described by Schmidt-Rohr and coworkers in 1999 (*5*), is ideally suited for studying slow motions in macromolecules. Stated simply, it is a one-dimensional chemical exchange experiment that relies on incomplete refocusing of a chemical shift anisotropy (CSA) echo based on molecular reorientation during a mixing time. Complete details have been explained previously (*10*, *11*), but the process is schematically represented by the pulse sequence shown in Figure 1 below which is applied under magic-angle spinning (MAS) conditions.

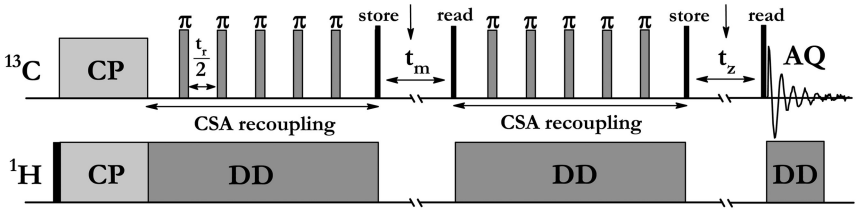

Figure 1. CODEX experiment pulse sequence applied under conditions of MAS. The value of the exchange mixing time t_m *ranges from 0.05 to 0.20 seconds for all data reported here. The total CSA evolution time corresponding to the sum of the first and second recoupling periods was* $2Nt_r$ *= (2)(4)(0.22 ms) = 1.76 ms. The* t_z *period, to ensure a constant time experiment, was 1 millisecond.*

It is important to note that the any dynamics which occur during the mixing time are events which are detected in real time, albeit indirectly based on their attenuation of the chemical shift echo. Although we have typically used mixing times t_m values ranging from 0.050 – 0.20 seconds, in theory this value could range widely, with an upper limit defined by spin-lattice relaxation. All ^{13}C and ^{1}H measurements were collected on a Bruker DSX-300 with field strength = 7.05T. The probe temperature was calibrated using $PbNO_3$ to within ±1 K. All CODEX exchange data was acquired with an actively-controlled MAS speed (typically 4-5 kHz), a 1-ms cross-polarization contact time, rotor synchronization, and as a precaution, CODEX measurements were altered between the CODEX and reference signal every 256 scans to eliminate spectrometer drift. In practice, one acquires a reference spectrum by interchanging the constant 1-ms t_z time with the mixing time. Since this time value is too short relative to slow chain dynamics, no motion can occur during such a short mixing period. This reference experiment yields a signal of maximum amplitude (S_o), which is then compared to the experiment where the much longer mixing time t_m is used (S). The normalized difference of the two experiments is referred to as the exchange intensity **E** = $(S_o - S)/S_o$, or $\Delta S/S_o$, which quantitatively reflects slow segmental dynamics. The exchange intensity **E** is a direct function of the length of the mixing time t_m, the characteric correlation time constant for whatever type of motion occurs (τ_c), and the temperature T. The complete equations describing the quantitative

In NMR Spectroscopy of Polymers: Innovative Strategies for Complex Macromolecules; Cheng, H. N., et al.;
ACS Symposium Series; American Chemical Society: Washington, DC, 2011.

relationship between **E** and these variables have been described in detail in previous publications (*7–11*). In all cases, ^{13}C spectra were analyzed.

We are cognizant of concerns arising from possible inhomogeneous polymer chain sampling based on experiments that begin with a cross-polarization step. While our primary interests revolve around very slow backbone chain dynamics at temperatures slightly below, near, and above the glass transition temperature (but much lower than terminal dynamics region), we do not wish to preferentially select chain segments that are much more rigid than the bulk. Rather, homogeneous sampling of all polymer chains in mixtures is desired. To address this concern in the context of amorphous polymer blends, we devised a modified version of the experiment employing only direct carbon polarization as the initial step in the experiment. Based on quantitative comparisons of the modified direct polarization versus CP-based CODEX results over a wide temperature range (including T_g) for atactic polypropylene (aPP), we demonstrated that results representative of all polymer chains in the sample are obtained in both experimental approaches (*12*). Therefore, we have confidence that CP-based CODEX-based exchange methods provide chain-level information representative of the bulk mixing and miscibility in amorphous macromolecules.

Results and Discussion

Using the experimental approach described above, one can extract exchange intensities E(T) versus temperature for chain specific locations, i.e., backbone CH_2 versus side-group CH_3. Whenever possible, signals from carbons in the backbone are used as reporters for slow segmental dynamics. In other cases, a methyl side group might be advantageous in that the signal is well-resolved from other signals once mixtures are formed. We will discuss examples from each approach in the following sections.

Figure 2 shows systematic comparisons of CODEX exchange intensities measured from backbone CH_2 versus side-group CH_3 in the two pure polymers (PEB and aPP) over the entire temperature range for which a measurable exchange signal is detected. This is an important control experiment, since it eliminates any uncertainty associated with additional side group dynamics that might influence the interpretation of the CODEX results in the blend, and their relevance to slow segmental dynamics. The onset of detectable exchange intensity for either functional group, as well as the temperature of the maximum E(T) value, is identical within each polymer. The absolute value of the maximum E(T) is markedly different for the backbone CH_2 vs. side-chain CH_3 signals in the PEB-66 polymer, indicative of additional ethyl branch motions which further reduce the magnitude of the chemical shift anisotropy for that pendant methyl group relative to backbone moeties, thereby decreasing E(T) values compared to the backbone CH_2. The exchange intensity for this CH_3 group in PEB-66 did increase, as expected, in experiments with longer recoupling times (not shown here). Since only a single carbon-carbon bond separates the CH_3 group from the main-chain in aPP, this dramatic difference in exchange intensity relative to the backbone is not observed. Two important points from this control experiment are:

In NMR Spectroscopy of Polymers: Innovative Strategies for Complex Macromolecules; Cheng, H. N., et al.;
ACS Symposium Series; American Chemical Society: Washington, DC, 2011.

(1) the temperature of the maximum E(T) value is independent of which group is measured, which means that the CH_3 signals can accurately report conformational exchange in the blend, an advantage given that they are better resolved than their respective CH or CH_2 backbone counterparts and can be deconvoluted accurately; (2) the onset of detectable E(T) signal in the CODEX experiment agrees with DSC data, in that the first one or two data points on the low temperature side of each curve coincide with the DSC T_g (PEB66 = 219 K and aPP = 262 K). Finally, in all cases a decrease in E(T) amplitude occurs when temperatures are high enough that thermally activated conformational rearrangements occur with a frequency larger than the magnitude of the CSA; this eliminates the possibility of detecting any signal differences between the exchange and reference spectrum since there is no longer orientation-dependent shielding information preserved in the system due to motional averaging.

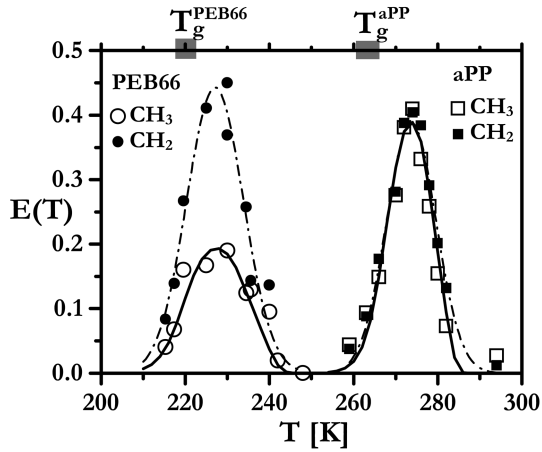

Figure 2. Normalized exchange intensities E(T) for methyl and methylene signals of pure PEB66 (a copolymer of ethylene and 66 wt% 1-butene) and pure aPP. The solid lines are Arrhenius model fits (see below) to the data, whereas the dash-dot lines are drawn through the methylene experimental points only to guide the eye. For reference, the Tg ranges via DSC are shown at the top of the figure. (Reproduced from reference (8))

From these example results, we observe that the CODEX experiment under MAS conditions provides dynamic information for slow chain reorientation/segmental motions on timescales similar to that probed by DSC methods, the latter being most familiar to practicing polymer scientists. However, as we will demonstrate in subsequent sections, and as has been described in detail in references 7-9, the overall information content and the chain specificity in mixed systems are much higher with the CODEX approach.

Figure 3 shows temperature dependent exhange intensities **E** for the same polymers described in Figure 2, and their miscible blend. We will use this miscible aPP/PEB-66 blend to illustrate the wide range of information (both model-independent and model-dependent) accessible using

In NMR Spectroscopy of Polymers: Innovative Strategies for Complex Macromolecules; Cheng, H. N., et al.;
ACS Symposium Series; American Chemical Society: Washington, DC, 2011.

the variable-temperature CODEX approach, and then conclude with brief representative results from other amorphous polymer blends. The data in Figure 3 represent the outcome of three independent temperature dependent experiments; one each for the two pure polymers and a single experiment for the blend from which polymer specific exchange intensities were extracted at each temperature. This latter point is important. In contrast to other experimental approaches, a single experiment on a mixed polymer system can provide data for all components in the mixture, which eliminates sample preparation uncertainties/reproducibility that often plague sequential methods where only one component may be analyzed in any one experiment (e.g., selective deuteration, dielectric spectroscopy, etc.)

Prior to any consideration of a quantitative model to fit the results, several key points may be discerned via simple inspection of the raw data in Figure 3, comparing the response of the ^{13}C signals in the CODEX experiment for each pure polymer to the response of that same polymer in the blend. First, the PEB66 exchange intensity curve shifts to higher temperature in the blend relative to pure chains (PEB66 is the lower T_g component). Similarly, the exchange intensity curve shifts to lower temperature for the aPP in the blend compared to its pure response. For the PEB66, the E(T) maximum shifts from 227 K to 247 K upon blend formation, while the aPP E(T) maximum changes from the pure value of 273 K to 253 K in the blend. Although each curve exhibits an identical 20 K change, they do not converge to an identical common value (5-7 K difference in E(T) maxima) even though the chains are intimately mixed. While omitted from the figure in order to maintain clarity, the E(T) versus T curve for the backbone CH_2 peak of aPP *in the blend* has a maximum at the same 252-253 K position as the CH_3 peak shown in Figure 3. Secondly, the breadth of each E(T) curve increases for either component in the blend relative to the pure polymer, especially for aPP. Finally, the absolute value of E(T) at each temperature across the detectable range decreases in the blend relative to the unmixed result for both polymer components. Although each temperature dependent exchange intensity curve decreases in intensity and increases in breadth for the polymers in the blend compared to the pure polymers, the overall integrated area under the curve fits (vide infra) remains constant for each polymer, within the error of the data analysis. While the intermediate temperature values for the E(T) curves are reminiscent of DSC results on blends, the ability to extract these specific details for each polymer in an amorphous mixture by simultaneous detection of the two unique E(T) curves is difficult using traditional thermal analysis methods. Typically, DSC traces on multicomponent miscible blends are broad and featureless, and one cannot discern individual behaviors for the polymer components. We conclude from these points that the overall dynamic heterogeneity for both polymer chains increases in the blend, and in addition, it is also known that the CODEX exchange intensity decreases with increasing number of sites involved in the exchange process for a fixed recoupling and mixing time (*11*). The details specifying exactly how the dynamic heterogeneity increases for both chains will be discussed in the following sections, and the reader can consult references 7-9 (and references therein) for additional details.

In NMR Spectroscopy of Polymers: Innovative Strategies for Complex Macromolecules; Cheng, H. N., et al.;
ACS Symposium Series; American Chemical Society: Washington, DC, 2011.

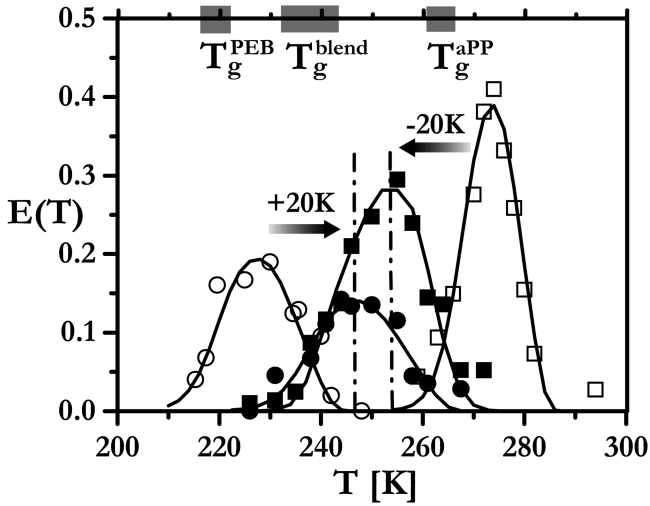

*Figure 3. Normalized exchange intensities **E(T)** for pure PEB66 (O), PEB66 in the blend (•), pure aPP (□), and aPP in the blend (■). The smooth lines are fits to the data using an Arrhenius model as described in the text. Note shifts of equal but opposite magnitude for each component upon blend formation, but a lack of complete convergence to a common temperature for the exchange intensity maximum of each polymer in the blend. The 5K/min scan DSC T_g range for each polymer and the blend is plotted for reference on the top of the figure, with the box length representing the beginning and end of the endotherm. (Reproduced from reference (8))*

Historically, the polymer science community espouses a miscible blend is characterized by identical Tg's for each polymer component in the miscible blend. While this can be true, it should not be taken as a criterion for miscibility, since Figure 3 above and Figure 8 (see below for further discussion of the PI/PVE miscible blend) clearly demonstrate that unique glass transitions (or "effective Tg's") can occur for constituent polymers in a miscible blend. Our results are in agreement with recent publications by Lodge discussing inequivalent Tg's for the polymers in miscible blends (*13*, *14*).

The fits to the experimental data shown in Figures 2 and 3 were obtained by combining isotropic rotational diffusion with a temperature-dependent discrete log Gaussian correlation time distribution/Arrhenius model (*15–19*). The absolute value of the exchange intensity E(T) at each temperature, for a fixed recoupling and mixing time, depends on the correlation time constant characteristic of the motion modulating the chemical shift anisotropy as well as the distribution of correlation time constants for all of the segments in the amorphous polymer or polymer mixture. We use a linear model that relates the width of the correlation time distribution to increasing temperature (*20*). Key results that can be obtained from the analyses include central correlation time constants for slow backbone reorientations in the pure and mixed systems (beginning from slightly below the glass transition to higher temperatures, but still in segmental dynamics regime), the

In NMR Spectroscopy of Polymers: Innovative Strategies for Complex Macromolecules; Cheng, H. N., et al.;
ACS Symposium Series; American Chemical Society: Washington, DC, 2011.

width of the correlation time constant distribution in both pure and mixed systems, and activation energies for segmental dynamics in the neat and blended polymers.

We recognize that other temperature dependent models may be more familiar to the polymer scientist. Figure 4 shows a comparison of the correlation time distribution/log Gaussian/Arrhenius model discussed above with a KWW/WLF analysis for the exchange intensity data from pure aPP and aPP in the blend; this is the same aPP raw data shown in Figure 3. The KWW/WLF fitting parameters are reported in the captions to Figures 4 and 5; we observe excellent agreement between the two models in terms of correlation time values over the temperature range of our data. Such low β values upon blend formation are consistent with increased dynamic heterogeneity in aPP,[11] as is apparent from direct inspection of the E(T) exchange curve intensities in Figure 3 and 4. Detailed comparisons of KWW β values to corresponding values of the correlation time distribution widths **g(τ)** are provided in the Supporting Information to Reference (*8*). That equivalent correlation times for the center of the distribution (τ_c) are obtained using either model is more clearly evident by the representation of their temperature dependence for both polymer components in Figure 5. One observes that the temperature dependence of the slow chain dynamics for PEB66 and aPP are very different. Figure 5 also shows that while the magnitude of the change in τ_c values upon blend formation differs between the two polymers significantly at any temperature (ca. 5 decade decrease in aPP versus ca. 2.5-3 decade increase in PEB66), the two polymer components *in the blend* have identical values of τ_c near 250 K.

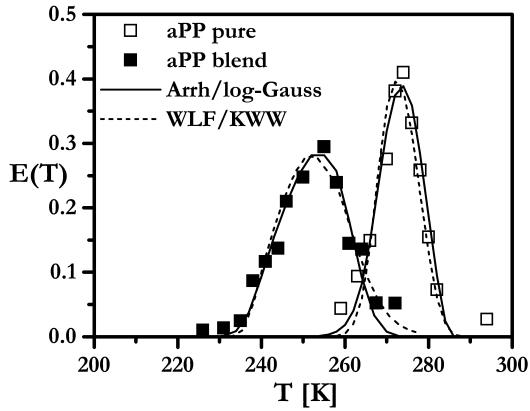

Figure 4. Comparison of fits to the aPP exchange data obtained using two different models: (1) Arrhenius temperature dependence of correlation times with variable-width log-Gaussian distribution, and (2) WLF temperature dependence combined with KWW distribution. The WLF/KWW parameters for pure aPP were C_1 = 15.5, C_2 = 41 K, $\tau(T_g)$ = 100 s, T_g = 259 K, β = 0.8, whereas for aPP in blend T_g = 237 K and β = 0.2 was used. (Reproduced from reference (8))

In NMR Spectroscopy of Polymers: Innovative Strategies for Complex Macromolecules; Cheng, H. N., et al.; ACS Symposium Series; American Chemical Society: Washington, DC, 2011.

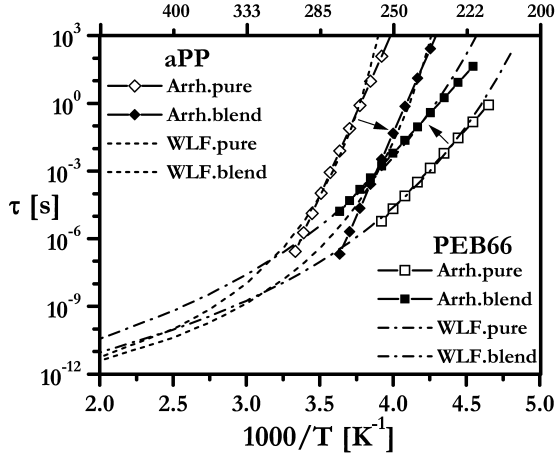

Figure 5. Temperature dependence of correlation times obtained using Arrhenius and WLF models for the aPP/PEB66 miscible blend. The WLF parameters for pure aPP were: C_1 = 15.5, C_2 = 41 K, $\tau(T_g)$ = 100 s, T_g = 259 K, whereas for aPP in blend T_g = 237 K was used. For pure PEB66 we used C_1 = 15.5, C_2 = 55 K, $\tau(T_g)$ = 100 s, T_g = 210 K, and the best fit for PEB66 in blend was obtained with C_2 = 68 K and T_g = 224 K. An Arrhenius model can be treated as linear approximation to the WLF curve, since both Arrhenius and WLF models give similar results over the temperature range for slow motions near Tg. (Reproduced from reference (8))

Figure 5 also clearly demonstrates that quantitative T_g timescales are revealed by these experiments, both for the pure polymers and the polymers in the blends. The correlation time constants for T_g in pure PEB and pure aPP both appear to be between 10 and 100 seconds (PEB near 10 and aPP nearer 100), but most importantly the data indicates that the change in T_g timescales, as well as their absolute values, for either component once the miscible blend is formed are quite different outside of a very narrow temperature range (250-260K).

Figure 6 shows calculated correlation time distributions from the fits to data in Figures 2 and 3 for the aPP component, demonstrating how the correlation time distribution function **g(τ)** can influence **E(T)** (*21*). We note how much broader the correlation time distributions become upon formation of the blend, and also, the increased distribution width near the T_g value (low T) for a pure polymer. By comparing Figures 5 and 6, we immediately observe that while central correlation time constants converge for each component in the miscible blend, albeit changing by largely different values, that the correlation time distributions actually diverge. Figure 6 shows that aPP, i.e. the high Tg component, becomes much more dynamically heterogeneous relative to its pure state, which is a common result for binary blends we have examined to date. Indeed, the total dynamic heterogeneity in the blend is much larger than the sum of the two unmixed polymer components, an important concept as one considers the thermodynamics of mixing in amorphous macromolecules (*vide*

In NMR Spectroscopy of Polymers: Innovative Strategies for Complex Macromolecules; Cheng, H. N., et al.;
ACS Symposium Series; American Chemical Society: Washington, DC, 2011.

infra). The reader may consult references 7-9 to see more detailed representations of correlation time distributions, and different schematics depicting their width as a function of temperature for pure and mixed states.

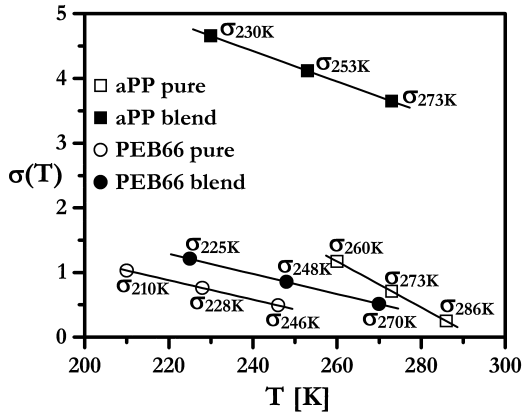

Figure 6. Temperature dependence of correlation time distribution widths σ for pure versus blended aPP and PEB66. (Reproduced from reference (8))

For brevity, only the variable temperature CODEX exchange curves are shown for two additional blend systems in Figures 7 (PIB/hhPP) and 8 (PI/PVE), along with fits to the raw data using the techniques described above. PIB/hhPP is unique among miscible blends we have studied to date in that the CODEX exchange curves do converge to the same value (as defined by onset of detectable exchange intensity, or more definitively by the maximum in the curve). If one determines the central correlation time constant for the temperature corresponding to the maximum in the E(T) curve, an identical value is observed for each polymer component in the blend. However, the change in segmental correlation time constants upon formation of the miscible blend is again much larger (by several orders of magnitude) for the high-Tg component hhPP than the low-Tg PIB component. Interestingly, the temperature where maximum exchange intensity occurs, as indicated by the vertical arrows in Figure 7, is 5-7 degrees lower than predicted by Gordon-Taylor/Fox equation mixing rules. In other words, it does not agree with composition-weighted average values, and qualitatively suggests an entropically driven mixing. Quantitative calculations based on central correlation time constants determined experimentally for the pure and mixed polymers, using the approach described here, confirm that positive configurational entropies of mixing exist for this blend, as well as other miscible polyolefin blends we have examined to date.

In NMR Spectroscopy of Polymers: Innovative Strategies for Complex Macromolecules; Cheng, H. N., et al.;
ACS Symposium Series; American Chemical Society: Washington, DC, 2011.

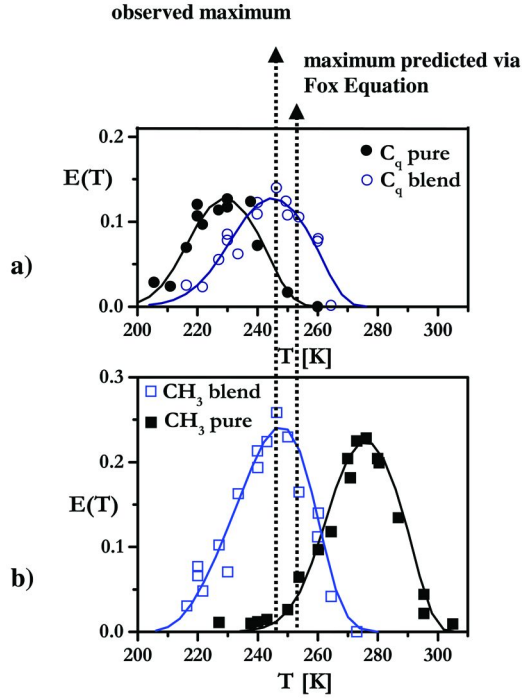

Figure 7. Normalized exchange intensities ***E(t$_m$)*** *for* ***a)*** *pure PIB measured at the quaternary backbone carbon (•) and PIB in the blend (o), and* ***b)*** *pure hhPP (■) and hhPP in the blend (□). Note the common exchange maximum temperature T=246 K for each polymer in the blend (left arrow) and the Fox equation prediction (right arrow). The smooth lines are fits to the data as described in the text. (Reproduced from reference (7))*

Figure 8 shows exchange curves for the PI/PVE miscible blend system. Note the apparent similarities between the general shape/location of the four curves and those in Figure 3, in that the curves for the polymers in the miscible blend do not converge to the same values (unlike the PIB/hhPP system in Figure 7). In total, these three results suggest that one cannot assume how slow segmental chain dynamics, which are the macromolecular dynamics most important for mechanical properties, change when a miscible blend is formed. Stated differently, one cannot assume that (a) a common glass transition will occur for the polymers in a miscible blend, and (b) composition-weighted averaged chain behavior takes place.

In NMR Spectroscopy of Polymers: Innovative Strategies for Complex Macromolecules; Cheng, H. N., et al.;
ACS Symposium Series; American Chemical Society: Washington, DC, 2011.

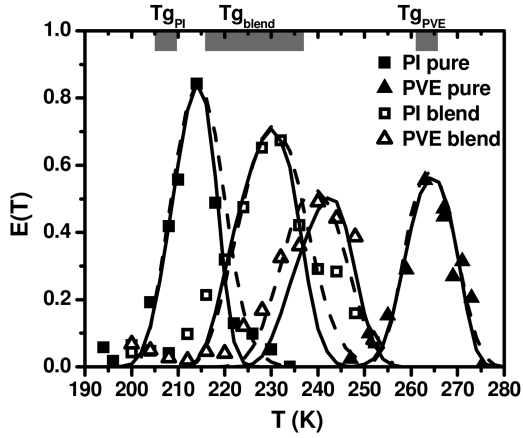

Figure 8. Normalized 200-ms exchange intensity ***E(T)*** *curves for pure PI and PVE and the same components measured independently in the blend. All data shown here reflect only backbone aliphatic carbons, not side chains or olefinic groups. The solid lines are fits to the data using an Arrhenius model with a variable-width log-Gaussian correlation time distribution. The dashed lines are fits to the data using the WLF/KWW model. The thick gray lines at the top of the figure indicate the 10 K/min DSC T_g range for the two pure polymers and the miscible blend. (Reproduced from reference (9))*

Complete quantitative analysis, using both Arrhenius and WLF/KWW models, of the data in Figures 7 and 8, including effective T_g's, central correlation time constants, correlation time distributions, and activation energies are reported in references (*7*) and (*9*). It is worth mentioning here that the PI/PVE system was an important control case as this blend has been studied by multiple investigators using a wide variety of techniques (*22–27*). However, as ours was the first method to get chain-selective information non-invasively from a single set of experiments on a single blend sample, we were pleased to find good agreement between quantitative data from our approach and selective deuteration techniques involving multiple blend preparations, as previously described (*26*, *27*). In addition to central correlation time constants, correlation time distributions, and activation energies, segmental friction coefficients were determined for each component in the PI/PVE system using a KWW/WLF treatment of the central correlation time data, where the characteristic segment length was taken as equal to the Kuhn length, or 1.1 nm.

In NMR Spectroscopy of Polymers: Innovative Strategies for Complex Macromolecules; Cheng, H. N., et al.;
ACS Symposium Series; American Chemical Society: Washington, DC, 2011.

During this review, we have deliberately pointed out model-independent and model-dependent conclusions accessible via the variable-temperature CODEX approach. Given that many of the key quantitative results come from fitting the raw E(T) data, it is appropriate to consider a mechanism by which the central correlation time constants τ_c can be evaluated independently.

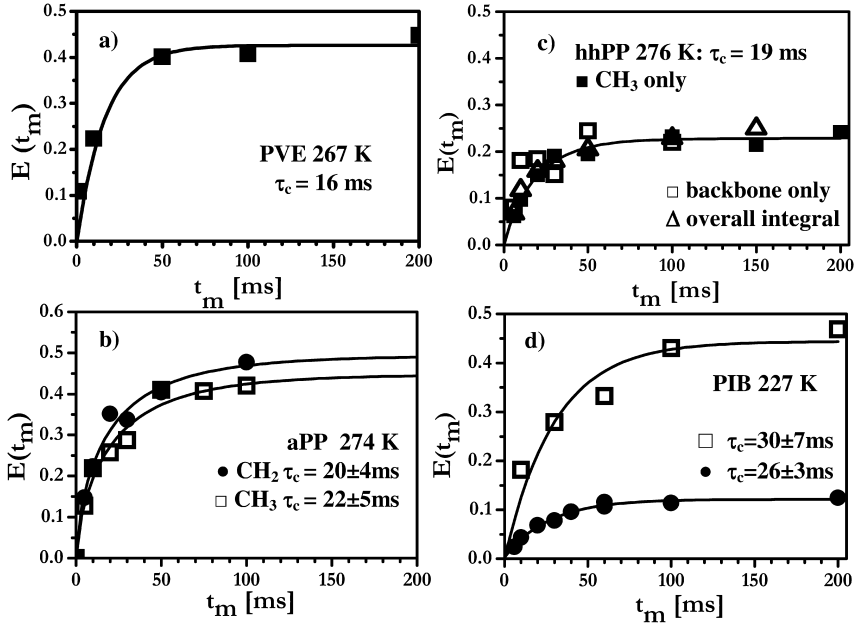

Figure 9. Exchange time constants extracted from an exponential fit to the rising exchange intensity curves are indicated on each of the Figures 9a-d for PVE, atactic PP (PP), head-to-head PP (hhPP), and polyisobutylene (PIB), respectively. For each of these same four polymers, at the same temperature as indicated on each plot, the respective central correlation time constants obtained from full analysis of the variable temperature exchange intensity curves of the type represented by the data in Figures 3, 4, 7, and 8, are: (a) τ_c = 14 ms (b) τ_c = 24 ms (c) τ_c = 20 ms (d) τ_c = 25 ms. The temperatures indicated in a-d are equal or very nearly equal to the exchange intensity maximum temperature for each polymer, resulting in similar values of τ_c. (Reproduced from reference (9)).

In Figure 9, we show results from such an independent evaluation, in which τ_c's were determined at temperatures near the maxima in the E(T) curves, using variable mixing time experiments for four different pure polymers including PVE, atactic polypropylene (PP), head-to-head polypropylene (hhPP), and polyisobutylene (PIB) at the indicated temperatures. The correlation time constants, extracted from an exponential fit to the rising intensity curve, are indicated on each of the Figures 9a-d, while values extracted from fitting the

In NMR Spectroscopy of Polymers: Innovative Strategies for Complex Macromolecules; Cheng, H. N., et al.; ACS Symposium Series; American Chemical Society: Washington, DC, 2011.

CODEX data are listed in the Figure 9 caption. (In figures where there are multiple data points, either multiple carbon positions in the polymer chain were probed, or as in Figure 9d, two different recoupling times in the CODEX experiment were compared.) The results in Figure 9 indicate that the correlation time constants obtained by full analysis of the raw data of the type shown in Figures 3, 4, 7, and 8 are accurate, with the largest difference for the polymers shown equal to 12% for PVE, and significantly less in the other three cases. While the time required to generate the experimental data in Figure 3, 7, or 8 is not trivial, such an approach is significantly shorter (by a factor of 5 to 10) than the time required to obtain full variable mixing time exchange curves, like those shown in Figure 9, over wide temperature ranges. This control experiment, as well as comparisons of PI and PVE data to previously reported correlation time values (*9*), indicate the quantitative robustness of our approach for macromolecular mixtures.

Given that we can calculate central correlation time constants characteristic of slow segmental reorientation for pure and mixed polymers over a wide temperature range, we can use the Adams-Gibbs formalism to quantitatively assess entropy changes that occur upon formation of a miscible blend (*28*). The relationship between configurational entropy $\mathbf{S_c}$ and $\boldsymbol{\tau_c}$ is:

$$\tau_c = \tau_o \exp(c/TS_c),$$

where we equate τ_c the value of the correlation time at the center of the distribution for either a pure polymer or the same polymer in a blend. Using data of the type shown in Figure 5, and assuming τ_o ranging from 10^{-12} s to 10^{-15} seconds and c as constant for each polymer in pure versus mixed state at a fixed temperature (usually taken as the temperature corresponding to maximum exchange intensity), we have determined that the total change in configurational entropy for PIB/hhPP and aPP/PEB-66 blends ranges from +10 to +20% upon formation of the miscible blend (and relative to the unmixed components). Therefore, one must conclude that an increase in the number of surface contacts either between dissimilar polymer chains or within chains themselves (an enthalpic model) in miscible polyolefin blends simply does not exist relative to the unmixed pure polymers. We view this as a conservative limit, since it does not quantitatively capture the large increases in the distribution of correlation times, or dynamic heterogeneity, associated with forming the miscible blend. The PI/PVE system is somewhat different in that it possesses sp^2 functional groups, and therefore free electron density which increases polarizability and induced association. Even so, Figure 10 clearly demonstrates that there is a slight positive entropy of mixing associated with forming the miscible blend, relative to the sum of the configurational entropy for the two unmixed components. The ability to non-invasively, selectively, and quantitatively determine this kind of data for amorphous polymers in a miscible mixture is a key advantage of this experimental approach.

In NMR Spectroscopy of Polymers: Innovative Strategies for Complex Macromolecules; Cheng, H. N., et al.;
ACS Symposium Series; American Chemical Society: Washington, DC, 2011.

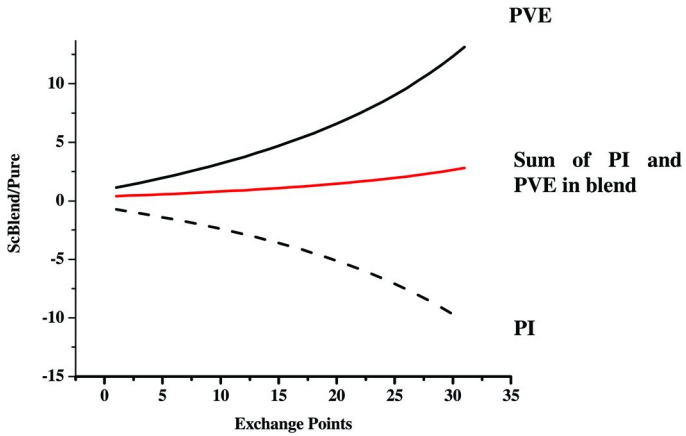

*Figure 10. Calculated values of the ratio of the total configurational entropy in the miscible blend to the sum of the pure component entropies (**S_c** Blend / **S_c** Pure), expressed in percent, versus the position on the exchange intensity curves shown in Figure 8 moving from low to high temperature. Each trace represents a calculation across the entire temperature range of the curve.*

Conclusions

A chain-specific experimental approach based on variable-temperature solid-state CODEX NMR experiments reveals that the effective glass transitions for each chain type in miscible blends may be inequivalent, and slow segmental dynamics for each polymer in the blend are characterized by unique central correlation times and unique correlation time distributions. Quantitative analyses of the raw data indicate that good agreement exists between effective Tg's, central correlation time constants, correlation time distributions, and friction coefficients extracted from this approach versus those obtained by other well-documented methods. Results from an isotropic rotation diffusion model with Arrhenius/log-Gaussian or WLF/KWW treatments of temperature dependence show clear sensitivity to changes that occur upon blend formation relative to the unmixed components. Positive configurational entropies of mixing are detected experimentally. That such quantitative information may be obtained for either polymer component in an amorphous mixture, without isotopic labeling, electric dipole moment constraints, or introduction of probe molecules, is a unique advantage of this experimental strategy and illustrates applicability to a wide range of multicomponent macromolecular systems beyond miscible blends, including polymer nanocomposites, organic/inorganic hybrids, biological macromolecules, and block copolymers.

In NMR Spectroscopy of Polymers: Innovative Strategies for Complex Macromolecules; Cheng, H. N., et al.;
ACS Symposium Series; American Chemical Society: Washington, DC, 2011.

Acknowledgments

The principal investigator gratefully acknowledges support from the National Science Foundation Division of Materials Research through grant DMR-0756291 and DMR-0611474.

References

1. National Science Foundation Report. *Interdisciplinary Globally-Leading Polymer Science and Engineering*, 2007, available via the Web at http://www.nsf.gov/mps/dmr/reports.jsp.
2. Ober, C. K.; Cheng, S. D.; Hammond, P. T.; Muthukumar, M.; Reichmanis, E.; Wooley, K. L.; Lodge, T. P. *Macromolecules* **2009**, *42*, 465.
3. Donald, A. M. *MRS Bulletin* **2010**, *35*, 702.
4. Frauenfelder, H.; Chen, G.; Berendzen, J.; Fenimore, P. W.; Jansson, H.; McMahon, B. H.; Stroe, I. R.; Swenson, J.; Young, R. D. *Proc. Nat. Acad. Sci. U.S.A.* **2009**, *106*, 5129.
5. deAzevedo, E.; Hu, W. G.; Bonagamba, T. J; Schmidt-Rohr, K. *J. Am. Chem. Soc.* **1999**, *121*, 8411–8412.
6. Wolak, J. E.; Jia, X.; White, J. L. *J. Am. Chem. Soc.* **2003**, *125*, 13660.
7. Wachowicz, M.; White, J. L. *Macromolecules* **2007**, *40*, 5433.
8. Wachowicz, M.; Wolak, J. E.; Gill, L.; White, J. L. *Macromolecules* **2008**, *41*, 2832.
9. Wachowicz, M.; Gill, L.; Damron, J.; White, J. L. *Macromolecules* **2010**, *43*, 3903.
10. deAzevedo, E.; Hu, W. G.; Bonagamba, T. J; Schmidt-Rohr, K. *J. Chem. Phys.* **2000**, *112*, 8988–9001.
11. deAzevedo, E. R.; Tozoni, J. R.; Schmidt-Rohr, K.; Bonagamba, T. J. *J. Chem. Phys.* **2005**, *122*, 154506.
12. Wachowicz, M.; Gill, L.; White, J. L. *Macromolecules* **2009**, *42*, 553.
13. Lodge, T. P.; McLeish, T. C. B. *Macromolecules* **2000**, *33*, 5278.
14. Haley, J. C.; Lodge, T. P. *J. Rheology* **2005**, *49*, 1277.
15. Wefing, S.; Kaufmann, S.; Spiess, H. W. *J. Chem. Phys.* **1988**, *89*, 1234.
16. Wind, M.; Brombacher, L.; Heuer, A.; Graf, R.; Spiess, H. W. *Solid State Nucl Magn. Reson.* **2005**, *27*, 132.
17. Kaufmann, S.; Wefing, S.; Schaefer, D.; Spiess, H. W. *J. Chem. Phys.* **1990**, *93*, 197.
18. Saalwachter, K.; Fischbach, I. *J. Magn. Reson.* **2002**, *157*, 17.
19. O'Connor, R. D.; Ginsburg, E. J.; Blum, F. D. *J. Chem. Phys.* **2000**, *112*, 7247.
20. deAzevedo, E. R.; Reichert, D.; Vidoto, E. L. G.; Dahmouche, K.; Judeinstein, P.; Bonagamba, T. J. *Chem Mater* **2003**, *15*, 2070.
21. See references 7−9 for discrete versus continuous plots illustrating this relationship.
22. Hefner, S.; Mirau, P. A. *Macromolecules* **1994**, *27*, 7283.
23. Roovers, J.; Toporowski, P. M. *Macromolecules* **1992**, *25*, 1096.
24. Roovers, J.; Toporowski, P. M. *Macromolecules* **1992**, *25*, 3454.

In NMR Spectroscopy of Polymers: Innovative Strategies for Complex Macromolecules; Cheng, H. N., et al.;
ACS Symposium Series; American Chemical Society: Washington, DC, 2011.

25. Alegria, A.; Colmonero, J.; Ngai, K. L.; Roland, C. M. *Macromolecules* **1994**, *27*, 4486.
26. Chung, G. C.; Kornfield, J. A.; Smith, S. D. *Macromolecules* **1994**, *27*, 964.
27. Chung, G. C.; Kornfield, J. A.; Smith, S. D. *Macromolecules* **1994**, *27*, 5729.
28. Adam, G.; Gibbs, J. H. *J. Chem. Phys.* **1965**, *43*, 139.